Inter-Comparison of Proximal Near-Surface Soil Moisture Measurement Techniques

Xiaoling Wu, Jeffrey P. Walker, *Fellow, IEEE*, François Jonard, and Nan Ye

***Abstract*—Precision agriculture is experiencing substantial development through the improved availability of cost-effective instruments for data collection. This includes ground-based proximal sensing technologies that are able to compete with satellite and aircraft observation systems, due to low operational costs, high operational flexibility, and high spatial resolution. This article was therefore designed to compare the performance of multiple sensing systems mounted on a smart buggy platform. A number of proximal sensing technologies were then evaluated and intercompared for their accuracy in retrieving high resolution near-surface soil moisture. The sensors tested included an *L*-band microwave radiometer (ELBARA III), a global navigation satellite system reflectometer sensor (LARGO), and an electromagnetic induction sensor (EM38). Data were collected during the fifth Soil Moisture Active Passive Experiment (SMAPEx-5) in Yanco, NSW, Australia, in September 2015. Observations from each sensor were converted to surface soil moisture values which were in turn evaluated against reference measurements obtained by *in situ* soil moisture measurements. The sensing technologies tested here have been individually assessed by many other studies, but within different regions and environments including surface condition, local weather, observing height, size of footprint, etc. Consequently, this article has used a single platform to intercompare the different sensors to be evaluated concurrently. Results from this article indicated that the *L*-band microwave radiometer achieved the best performance in retrieving surface soil moisture. The average RMSE and *R* were found to be 0.055 cm^3/cm^3 and 0.68 for ELBARA III, 0.084 cm^3/cm^3 and 0.51 for LARGO, and 0.090 cm^3/cm^3 and 0.32 for the EM38.**

***Index Terms*—Passive microwave, precision agriculture, reflectometry, soil moisture.**

I. Introduction

WATER in the soil governs the energy and hydrologic cycle of the Earth, thus impacting floods and droughts [1], [2]. Moreover, agriculture productivity is heavily constrained by the amount of water in the soil, and in turn water use efficiency strongly impacts crop yield and the amount of irrigated crop area that can be farmed [3]–[6]. Accordingly, new sensing technologies are at the cusp of providing a state-of-art infrastructure to farmers that will allow them to precisely monitor their crop water requirements spatially, so as to optimize their irrigation scheduling and agricultural productivity.

Water is a scarce resource that limits the amount of land which can be irrigated, so even a small water saving through optimized application rates will allow more land to be irrigated. Moreover, under- or overwatering can have significant environmental impacts, ranging from water logging to vegetation stress, with both having a significant impact on crop yield. Access to real-time data on the soil moisture content will therefore allow growers to control their water application rates. Thus, a system with the ability to accurately monitor the soil moisture distribution will not only lower the per-hectare costs of production, but also raise yield and in turn maximize profit. However, soil moisture is spatially variable and in-situ field measurements on a large scale are very time consuming and costly. While soil moisture stations can provide long-term measurements, they typically do not represent the spatial variation. Although the sensors onboard satellites are capable of monitoring soil moisture across large scales, they suffer from spatial discontinuity and spatial resolution [7]–[13]. Together, these limitations have forced the development of innovative proximal sensing technologies for capturing the spatial distribution in near-real-time at local scale. This article was therefore designed to test multiple proximal sensors mounted on a "buggy" platform for their skill in retrieving spatio-temporal soil moisture, and thus select the one with the greatest potential to save water and boost the crop yield in future agricultural applications. With the aid of this state-of-art sensing technology, irrigators will be more inclined to irrigate when the crops need water, not just when it suits the irrigator, so as to fulfil more viable farming practices as well as an improved lifestyle.

The "buggy" used in this article is an all-terrain tractor with a size of 3.5 m $\times$ 1.2 m and a speed up to 40 km/h. This platform provided the first-ever opportunity to directly inter-evaluate the performance of different types of proximal sensors for spatial soil moisture retrieval at local scale. The sensors investigated here include the *L*-band microwave radiometer (ELBARA III), the light airborne reflectometer for global navigation satellite systems reflectometry (GNSS-R) observations (LARGO), and an electromagnetic induction (EM38) sensor. While considerable effort has been focused on the development of each unique sensing technology separately, it is now recognized that the next significant advance in agricultural application, especially

Manuscript received October 6, 2021; revised December 9, 2021 and February 9, 2022; accepted February 25, 2022. Date of publication March 7, 2022; date of current version March 23, 2022. This study was performed within the SMAPEx framework. The SMAPEx field campaigns and related research development have been funded by Australian Research Council Discovery under Grant DP0984586 and Grant DP140100572 and Infrastructure under Grant LE0453434 and Grant LE0882509. *(Corresponding author: Xiaoling Wu.)*

Xiaoling Wu, Jeffrey P. Walker, and Nan Ye are with the Civil Engineering, Monash University, Clayton, VIC 3800, Australia (e-mail: xiaoling.wu@monash.edu; jeff.walker@monash.edu; nan.ye@monash.edu).

François Jonard is with the Agrosphere (IBG-3), Institute of Bio- and Geosciences, Forschungszentrum Julich GmbH, 52428 Julich, Germany (e-mail: f.jonard@fz-juelich.de).

Digital Object Identifier 10.1109/JSTARS.2022.3156878

Fig. 1. Buggy platform with multiple sensors, including: an *L*-band microwave radiometer (ELBARA III), a GNSS-R sensor (LARGO), an electromagnetic induction sensor (EM38), a thermal infrared radiometer, multispectral (VIS/SWIR) sensors and INS, control and power units. Unfortunately technical issues have precluded use of data from the optical instruments in this comparison.

in water consumption, will come from a careful selection from viable sensors tested concurrently.

II. Instrumentation and Study Area

A. L-Band Microwave Radiometer (ELBARA III)

ELBARA III (third generation), developed by the European Space Agency (ESA) for the soil moisture and ocean salinity (SMOS) calibration and validation activities, is a ground-based *L*-band microwave radiometer [14], [15]. The ELBARA radiometer has already been successfully used in several hydrological studies on a mobile platform [16], [17] or a tower [18], [19]. It measures brightness temperature (TB) for vertical and horizontal polarizations within the protected frequency band 1400–1427 MHz. Microwave radiometery at *L*-band has been studied broadly and considered as the most promising remote sensing technology for surface soil moisture retrieval [20], [21]. Due to its all-weather capability and direct relationship with soil moisture through the soil dielectric constant, it has been adopted for monitoring soil moisture conditions globally, through satellites, such as ESA's SMOS mission and NASA's soil moisture active passive (SMAP) mission [21], [22]. However, the spatial resolution of these data is around 36 km making it unsuitable for precision agriculture. Consequently, application of this technology on aircraft or a buggy provides the opportunity to significantly enhance the resolution to that which can be applicable to agriculture by being closer to the ground. Accordingly, the horn antenna of ELBARA III was situated on a 2.2-m high bar on top of the buggy (see Fig 1) to provide a spatial resolution of approximately 3 m. The angle of the horn is adjustable, however an angle of 40° was used in this article replicating that of the SMAP mission, which was found to have a retrieval accuracy of 0.021 cm^3/cm^3 and correlation coefficient R of 0.62 at 9 km resolution when using the optimal retrieval algorithm [23].

B. Light Airborne Reflectometer for Global Navigation Satellite Systems Reflectometry Observations (LARGO)

The LARGO was initially developed as an airborne instrument designed for measuring the coherent reflectivity from different soils. In this article, LARGO was used in a field campaign mounted on the buggy together with other conventional remote sensing instruments. GNSS-R is a promising tool for Earth observation. It was first proposed in 1993 for satellite mesoscale altimetry [24], but since the mid 90's several other applications have appeared, such as sea state [25], snow [26], and soil moisture [13], [27]–[29] monitoring, among others. The LARGO reflectometer is a dual-channel instrument: one channel acquires the direct GNSS signals with a right-hand circular polarization (RHCP) active antenna while the other channel acquires the reflected GNSS signals with a left-hand circular polarization (LHCP) active antenna, since GNSS signals for elevation angles higher than 30° become LHCP after reflection [30]. This article inverted measured coherent reflectivity using LARGO to corrected coherent reflectivity (through antenna pattern compensation and a topographic correction) that ultimately provided the soil moisture retrieval. Fig. 1 shows the LARGO installation with the up-looking and down-looking antennas mounted on ground planes near the front of the top bar. Due to the mounting positions of ELBARA and LARGO, they have an almost overlapped footprint with a size of approximately 3 m in diameter.

C. Electromagnetic Induction Sensor (EM38)

Electromagnetic Induction (EMI) has potential advantages over other methods for soil moisture monitoring including speed and ease of use, no radioactive source, and its noninvasive nature. Use of the EM38 does not require wiring, electronic equipment or access tubes to be installed into the field. For these reasons, the EMI technique has been developed to enable managers/farmers to repeatedly monitor a large number of sites over an extended period in cropped fields. EMI provides a measure of the soil electrical conductivity (EC) of the soil profile, which is affected by variation in salt, clay content, organic matter, temperature, and soil moisture. Therefore, through careful selection of sites, and consistent reading of the same sites, the impacts of spatial variation of clay, salt and organic matter upon conductivity measures can be avoided [31]. The remaining variation in EMI measurements correlates strongly with variation in soil moisture. This instrument can therefore provide a rapid method for estimating soil moisture content at a large number of field locations.

An EM38 is one example of an EMI device. It contains two coils of wire: one for creating a magnetic field (transmitter coil) and the other for sensing an external magnetic field (receiver coil). The receiver coil is tuned to measure the strength of the induced magnetic fields which is then converted to a measure of the apparent EC (ECa) in the soil, with the ECa changes over time dominated by the soil moisture changes [32], [33]. The EM38 instrument was towed behind the buggy as shown in Fig. 1.

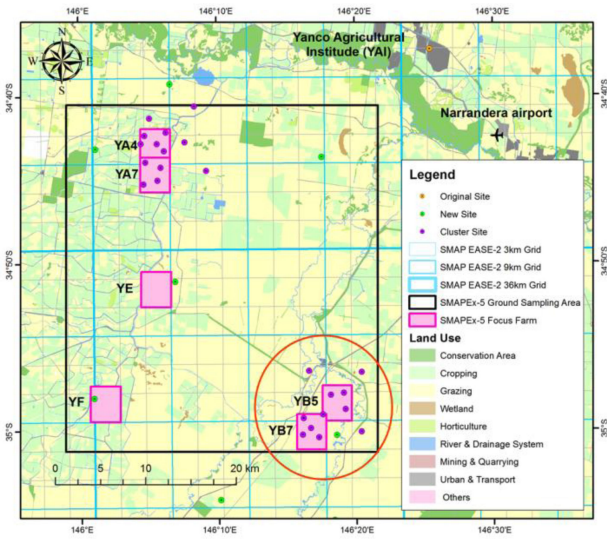

Fig. 2. The fifth soil moisture active and passive experiment (SMAPEx-5) study site; the grassland YB in the red circle is the experimental area for this article where buggy observations were taken.

Fig. 3. Example of the buggy driving route across YB area (left), dominant land cover type-grass (right-bottom), and some flooded area within YB (right-top).

D. Buggy Platform

Apart from ELBARA III, LARGO, and EM38, there were also other instrument on board this buggy: a field laptop for sensor control and visualisation of buggy position; thermal and spectral sensors for providing surface temperature; and vegetation index, an inertial navigation system (INS) for navigation on the laptop; and batteries for running all the sensors. This buggy is easy to control and drive over various off-road conditions, however in this application the driving speed was constrained to no more than 5 km/h, thus providing a reasonable number of samples for averaging to 50 m spatial maps.

E. Study Area and Data Description

This article was conducted within the framework of the fifth SMAP experiment (SMAPEx-5) [34]. The SMAPEx-5 field campaign was carried out in the Yanco area of New South Wales in Australia from September 7–27, 2015 (see Fig. 2). The SMAPEx field campaigns were specifically designed to collect airborne active and passive microwave data, ground observations of soil moisture, and ancillary data needed for soil moisture retrievals in coincidence with NASA's SMAP coverage, providing microwave observation and soil moisture references for SMAP in-orbit validation. The SMAPEx study site is within a semiarid agricultural and grazing area located in the Murrumbidgee River catchment in south-eastern Australia (-34.67˚N, -35.01˚N, 145.97˚E, and 146.36˚E), and forms part of the greater Murray–Darling basin. A general description of the SMAPEx study area and monitoring activities can be found in [34], with full details of the experiments available in the experiment plans on the SMAPEx website.[1]

The YB area as shown in Fig. 2 was the place where the buggy runs took place, dominated by grassland with mostly flat topography (see Fig. 3). The field campaign commenced with very moist soils which were partially flooded and thus not accessible, and dried down over the course of the three week long experiment. Due to the impact of localized inundation the driving route was constrained to avoid the flooded area. Fig. 3 shows an example of the driving route.

The field data used in this article include: TB at *h*- and *v*-pol acquired by ELBARA III; ECa obtained by EM38; and coherent reflectivity from LARGO, all resampled to 50 m resolution; destructive vegetation sampling and surface roughness from a roughness profiler were also used as ancillary data inputs to the soil moisture retrieval model. Intensive soil moisture measurements sampled at 50 m resolution by a hand-held hydraprobe data acquisition system (HDAS; [35]) was used as the reference for retrieved soil moisture from the different proximal sensors.

This article was performed over five days from SMAPEx-5: September 9, 11, 17, 22, and 27, 2015. The daily activities mainly included cold and warm calibration for ELBARA III, calibration of EM38, and buggy driving by following the prepared routes, data collection from each sensor, data download and archiving at end of each day. Due to the driving limitations and occasional malfunction of some sensors, only the overlapping area with data from all sensors and dates has been selected for evaluating the performance of each sensor.

III. Methodology

A. ELBARA III Soil Moisture Retrieval

Current algorithms for passive microwave soil moisture retrieval are based on inversion of a radiative transfer model that simulates the passive microwave emission from the land surface using ancillary information such as vegetation-related indices, soil surface roughness, and soil temperature [36]–[38]. The *L*-band microwave emission of the biosphere (L-MEB) model [39], developed for the SMOS mission, was used here. The core of this model is based on the well-known *tau–omega* model in the passive microwave soil moisture community. This model is also

[1] [Online]. Available: www.smapex.monash.edu.au

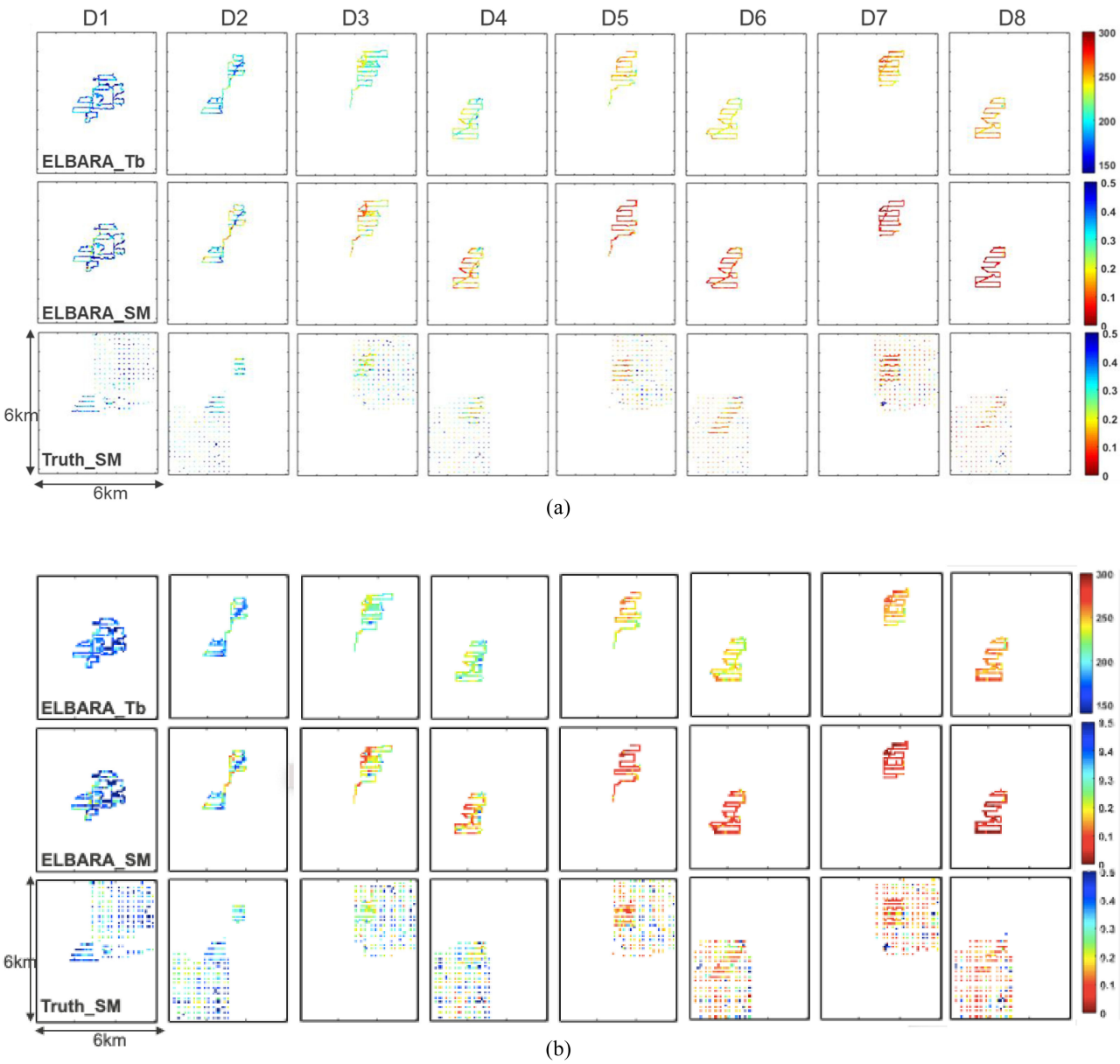

Fig. 4. Spatial plots of ELBARA TB at h-pol (in Kelvin), ELBARA retrieved soil moisture (in cm^3/cm^3), and the ground truth soil moisture (in cm^3/cm^3) across eight days during the SMAPEx-5 campaign. TB at both h-pol and v-pol were used in this article, but with only the one at h-pol shown in Fig. 4 as an example. Data shown here are at (a) 50 m and (b) 100 m resolution, respectively.

applied in the SMAP level 2 passive microwave soil moisture algorithm [40].

The *tau–omega* model requires two main parameters to represent the vegetation attenuation properties and the scattering effects within the canopy layer: the optical depth of the canopy τ and the single-scattering albedo ω, which are used to parameterize the vegetation attenuation properties and the scattering effects within the canopy layer. The basic concept of the *tau–omega* model has been illustrated in [38] and the detailed description of the model equations used in this article can be found in both [39] and [40]. Apart from τ and ω, other model parameters include a soil roughness parameter *HR* and vegetation parameter *b*. *HR* was obtained using a pin profiler as explained in [38]. The optical depth τ has been linearly related to the vegetation water content (VWC) using the empirically fitted *b* parameter through

$$\tau = b * \mathrm{VWC}. \tag{1}$$

The effective soil temperature required in the model can be calculated using near-surface (2–5 cm) temperature T_{SURF} and deep-soil temperature (~50 cm) T_{DEEP} (from a nearby *in situ* station) from

$$T_{\mathrm{EFF}} = T_{\mathrm{DEEP}} + (T_{\mathrm{SURF}} - T_{\mathrm{DEEP}}) * (\theta / w_0)\, b_0 \tag{2}$$

where θ is the surface soil moisture, and $w_0 = 0.398$ and $b_0 = 0.181$ are semiempirical parameters depending on specific soil characteristics that were calibrated by Wigneron *et al.* [39].

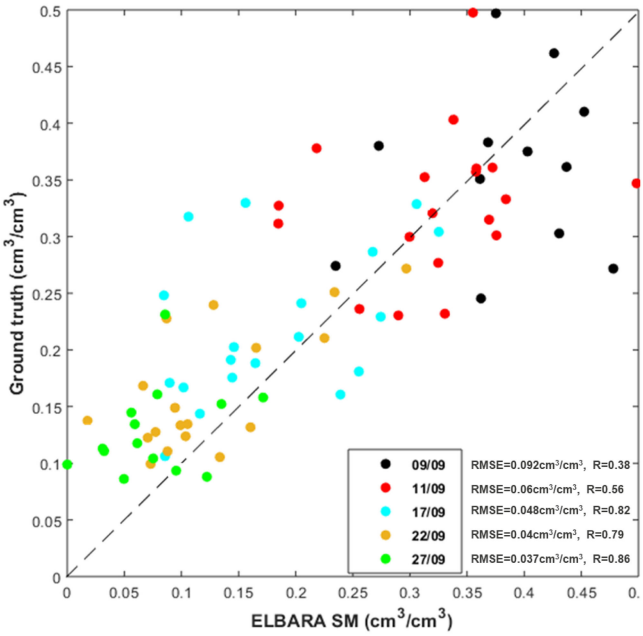

Fig. 5. Comparison between ELBARA retrieved soil moisture and ground truth across five days: September 9, 11, 17, 22, and 27, 2015.

The vegetation temperature T_{VEG} required in the model was considered to be equal to T_{SURF}.

B. LARGO Reflectivity Estimation and Soil Moisture Retrieval

Considering the bistatic radar equation and the fact that for a bare soil surface the coherent component dominates against the incoherent component, the reflectivity from RHCP transmission and LHCP reception can be estimated by

$$\widehat{\Gamma_{\mathrm{RL}}} = \beta \cdot \frac{G_{R_D}(\theta,\phi) \cdot \rho_D(\theta,\phi) \cdot \mathrm{SNR}_R}{G_{R_R}(\theta,\phi) \cdot \rho_R(\theta,\phi) \cdot \mathrm{SNR}_D} \tag{3}$$

$$\beta = \frac{T_{A_R} + T_{R_R}}{T_{A_D} + T_{R_D}} \tag{4}$$

where β is a correction factor due to the different antenna and receiver's noise temperature, $G_{RD}(\theta,\phi)$ and $G_{RR}(\theta,\phi)$ are the antenna gain for the direct and reflected signal channel, respectively, θ and ϕ are the antenna coordinates which indicate where the input signal is coming from, $\rho_D(\theta,\phi)$ and $\rho_R(\theta,\phi)$ are the polarization mismatch factor between the incoming signal and the antenna polarization coefficient for the direct and reflected channels respectively, SNR_D and SNR_R are the signal to noise ratio computed at the reflectometer back-end receivers for the direct and reflected channels, T_{AR} and T_{AD} are the antenna noise temperature for the reflected and direct channels, and finally, T_{RR} and T_{RD} are the receiver's equivalent noise temperature for the reflected and direct channels respectively. Thus, the reflectivity of LARGO can be estimated. More detailed description on this equation can be found in [41].

LARGO reflectivity can be compared with the actual ground soil moisture value (the intensive soil moisture sampling from the SMAPEx-5 field campaign). Such comparison allows for a rapid evaluation of LARGO over the study area and thus demonstrate the possibility of using GNSS reflections to observe the surface soil moisture. Based on the sensitivity derived via linear regression with ground truth, the corresponding soil moisture values can be converted from reflectivity. The average of ground truth is also computed to reference the LARGO-based soil moisture to an absolute scale.

C. EM38 Soil Moisture Estimation

The measured ECa is an accumulated value affected by the whole soil profile (from surface to 1.2 m deep). Assuming the dominant driver of local EC is soil moisture, the EC at depth z, EC(z), is directly proportional to the volumetric moisture content at this depth $\theta_v(z)$. This assumption is reasonable in a situation where the concentration of soluble salts is constant with depth. Thus, the EM38 response should be proportional to the addition of the combined depth response function [42], [43] and θ_v according to

$$EC_{a(\mathrm{measured})} \approx k \sum_{z} \theta_v(z) \times \varphi^V(z) \tag{5}$$

$$\varphi^V(z) = \frac{4z}{(4z^2+1)^{3/2}} \tag{6}$$

where z is the ratio of axial distance below the sensor and inter-coil spacing (1m), $EC_{a(\mathrm{measured})}$ is the EM38 integrated response in mS/m, k is the constant of proportionality between EC and θ_v at the same depth z, assuming the relative contributions of all other EC-driving parameters remain fixed at depth, and $\varphi^V(z)$ is the depth response function for either vertical or horizontal dipole orientation (vertical dipole was adopted in this article). Theoretically, soil moisture at different depths are able to be estimated given a large amount of *in situ* sampling for calibrating the procedure. However this is hardly ever achieved due to the time and labour cost and thus was out of the scope of this article. Consequently, for this article it was further assumed that the integrated ECa from the EM38 is only related to the near-surface soil moisture. Therefore the derived soil moisture from ECa was obtained from a linear regression with the ground truth. As the slope varies each day individual calibration was conducted on a daily basis.

IV. Results and Discussion

This section will be elaborated in the following parts: relationship between ELBARA-derived soil moisture; LARGO-derived soil moisture; EM38-derived soil moisture; and the ground reference.

A. ELBARA-Derived Soil Moisture

The TB data was calibrated and geo-referenced across the eight days of SMAPEx-5. Fig. 4 displays the temporal variation of TB at h-pol across those days which clearly shows a drying-down period, starting from an average of 170 k at the beginning to 255 k at the end of the campaign. After running the *tau-omega* model by inputting TB and ancillary data, the soil moisture maps were generated as shown in the middle of Fig. 4, showing the soil moisture drying-down trend, from 0.40 to 0.053 $\mathrm{cm}^3/\mathrm{cm}^3$.

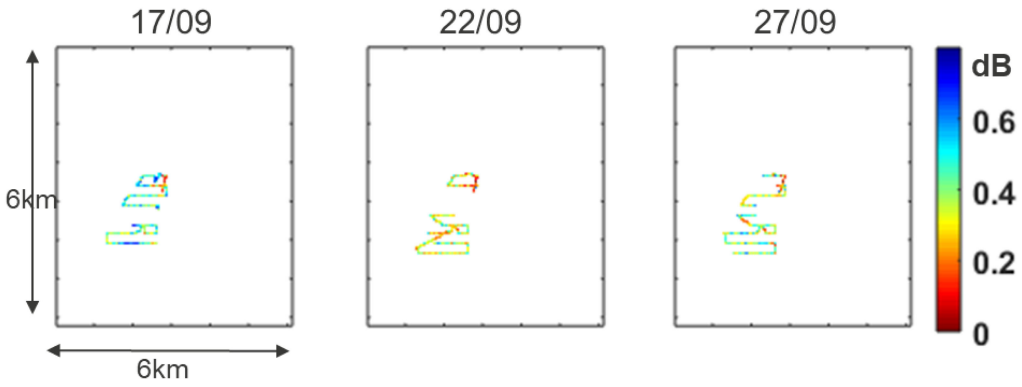

Fig. 6. Spatial plot of Largo corrected reflectivity (in dB) across three days (September 17, 22, and 27, 2015) during SMAPEx-5.

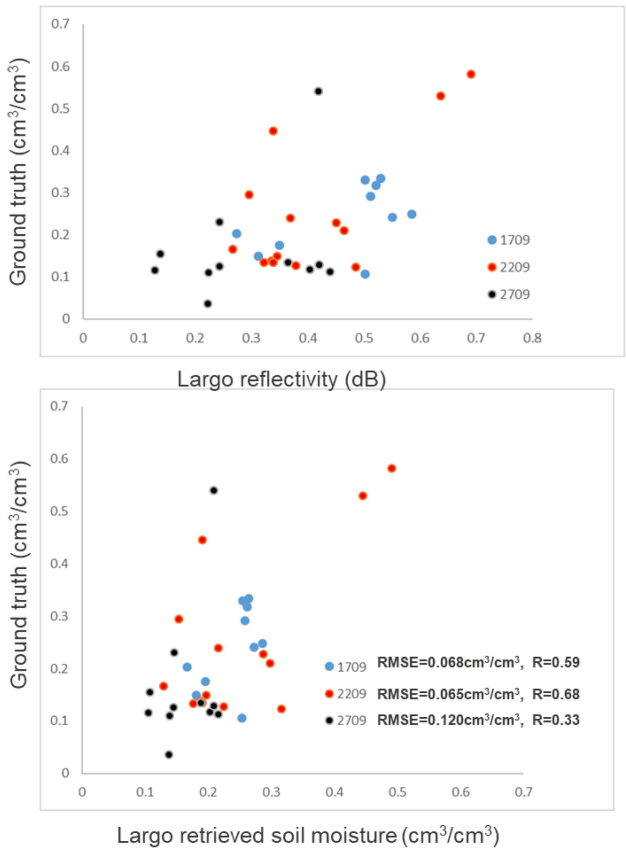

Fig. 7. Comparison between ground truth and Largo reflectivity (top) and Largo retrieved soil moisture (bottom) across three days: September 17, 22, and 27, 2015.

The ground reference soil moisture map was obtained from two sources: 250 m spacing and 50 m spacing sampled data, both from the hand-held HDAS described earlier. The 250 m resolution points were initially designed for calibration and validation of airborne observation, while the 50 m resolution points were added specifically for the buggy research, but with smaller coverage. Both lots of soil moisture data were combined to a 50 m map as a ground reference for evaluating the accuracy of the proximal sensors on the buggy. Spatial maps of the ground reference can be found in the bottom row of Fig. 4. As mentioned previously, daily coverage for each sensor differed due to occasional malfunction, and therefore only the overlapping areas of the sensors on five days (September 9, 11, 17, 22, and 27, 2015) could be inter-compared, being a $\sim$1 km $\times$ 1 km size area within the YB7 site. Therefore, correlation between ELBARA-derived soil moisture and the ground reference across these five days and the restricted coverage has been analysed with the scatterplot shown in Fig. 5. The poorest performance was found on the September 9, with a bias of 0.035 cm^3/cm^3, RMSE of 0.092 cm^3/cm^3, and correlation coefficient R of 0.38; while the last day 27th achieved the best performance with a bias of 0.016 cm^3/cm^3, RMSE of 0.037 cm^3/cm^3, and R of 0.86. The average RMSE and R across the five days was 0.055 $cm^{3/}cm^3$ and 0.68. The performance improvement across the dry-down was possibly due to flooded surface, with large differences between derived soil moisture and ground measurements around the flooded and muddy areas. The samplers with hand-held HDAS had to choose nearby unflooded points to represent the value of that particular flooded area while ELBARA mounted on the front long bar took continuous measurements along its path, including for flooded and muddy areas. When those areas became more accessible for ground measurement the errors over those pixels decreased accordingly.

B. LARGO-Derived Soil Moisture

Reflectivity in dB was obtained through direct and reflected signals and compensated by their corresponding antenna patterns. Maps of reflectivity across the three days (September 17, 22, and 27, 2015; data on 9th and 11th were not included here due to the malfunction of the sensor which has resulted in very limited points being covered and therefore being statistically insignificant) are displayed in Fig. 6. High reflectivity is associated with high water content whereas low reflectivity means low water contents. To this extent, there is a trend from the relatively high reflectivity on 17th to the low reflectivity at the end of the campaign, being similar to the trend of ground reference soil moisture transition. Correlation coefficient between reflectivity and ground truth was calculated and the regression function shown for each day in the upper row of Fig. 7. The highest correlation was found on the September 22, being around 0.68, followed by the September 17, with around 0.52. The correlation

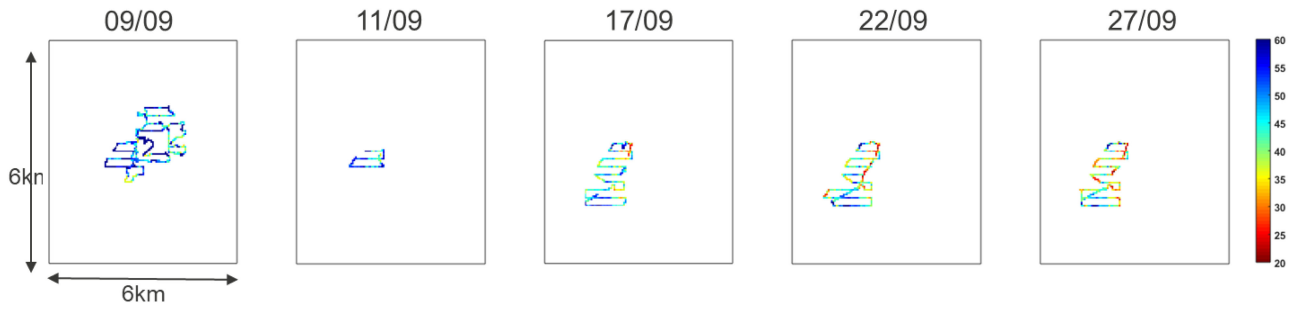

Fig. 8. Spatial plot of EM38 conductivity (in mS/m) across five days (of September 9, 11, 17, 22, and 27, 2015) during SMAPEx-5.

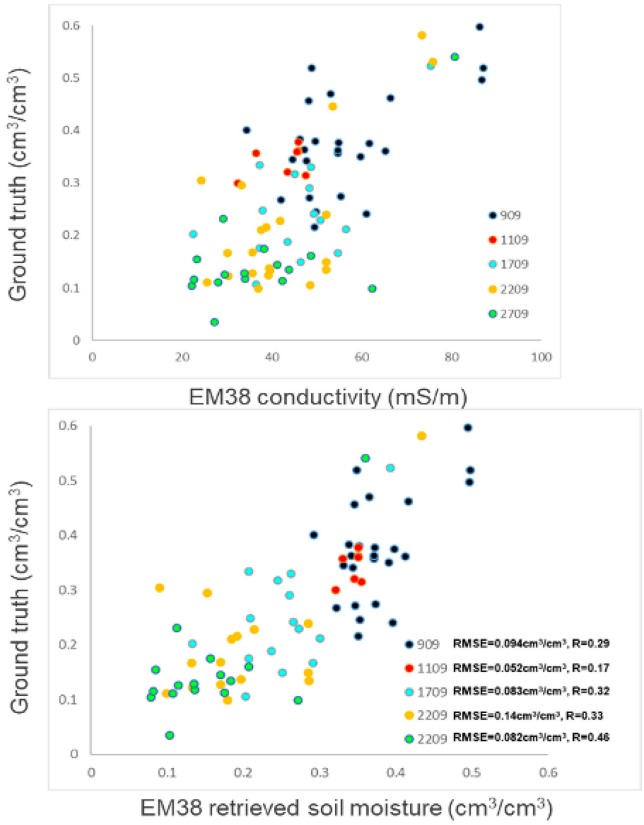

Fig. 9. Comparison between ground truth and EM38 conductivity (top) and EM retrieved soil moisture (bottom) across five days: September 9, 11, 17, 22, and 27, 2015.

on the September 27, was very low ($R = 0.32$), in contrast to ELBARA, possibly due to the dry conditions near the end of the field campaign. This is expected, as when the soil is dry the detection depth of the GNSS-R signal can be deeper than 20 cm and thus cause larger difference to the ground reference measured for only the top 5 cm. Based on each regression function a soil moisture map was derived from LARGO observations and then further compared to the ground reference. As seen from Fig. 7, data from the September 22, had the best performance with RMSE and R being 0.065 cm^3/cm^3 and 0.68; the poorest result was found on the September 27, being 0.120 cm^3/cm^3 and 0.33. The averaged correlation R between derived soil moisture and ground truth across the 3 days was 0.51, and the averaged RMSE was 0.084 cm^3/cm^3, being poorer than the results from ELBARA. In this instance, not only were results affected by the flooded condition, but also by the very dry conditions.

C. EM38-Derived Soil Moisture

For this sensor, the soil moisture was derived from the EC through a simple calibration procedure, based on the assumption that the variation of ECa is dominated by variation in the soil water content, and the assumption that the integrated ECa is directly correlated to the near-surface layer soil moisture. Therefore, linear regression was carried out for each day and the function applied to the measured conductivity to retrieve the soil moisture. Fig. 8 shows the spatial maps of EC across the five days at 50 m resolution; here high conductivity values indicate a wet condition while low conductivity means dry surface. Again a drying-down trend was observed from the EM38 conductivity, starting from an average of 54 to 38 mS/m at the end. A regression function was computed for each day from the correlation between conductivity and ground soil moisture as displayed in Fig. 9 together with the correlation coefficient.

For EM38, the best correlation was found on September 27, when the R was 0.46; the worst was on 11th with an R of $\sim$0.17. By comparing with the ground reference, it was found that on the September 27, that the EM38 conductivity showed an agreement in spatial patterns across the site; while on the September 11, there were contradictory results over some parts of the site. However, lack of enough EM38 points on the September 11, was also an issue. After applying the linear regression to the observed conductivity, the soil moisture map was derived for each day and evaluated against the ground truth as illustrated in Fig. 9. Although the derived soil moisture showed a consistent drying-down trend, larger variation on derived soil moisture across the site was found for almost each day. The overall performance of the EM38 was found to be poor according to the RMSE and R values, with an average RMSE of 0.090 cm^3/cm^3 and R of 0.32. These relatively poor results are potentially a result of the assumptions made in this analysis.

V. Conclusion

Water conservation techniques in farms save not only water, but money, time, and effort, as well as benefiting the natural environment. Making irrigated agriculture more productive not only increases production, but also creates more jobs, as more

water efficiency means more land can be irrigated and therefore as a result of the increased work more jobs are created. A buggy has been implemented as a platform to represent farm vehicles used to conduct routine farm management operations, including ploughing, fertilizing, harvesting, and or moving cattle. Accordingly, it was used to test and intercompare a range of available proximal remote sensing methods that can be used for high resolution mapping of soil moisture across farms. ELBARA III, an *L*-band radiometer, had the best performance in this article, proving its ability to be included in future smart farm management and/or irrigation systems, which can play an enormous role in contributing to fresh water savings. Future studies will include the development of a lighter and more cost-effective *L*-band radiometer to be mounted on a UAV, with the aims not only to maintaining the accuracy of *L*-band radiometer in retrieving soil moisture, but also making a more reliable and affordable smart platform to be used by the farmers.

In comparison to other proximal sensors for soil moisture retrieval, the ELBARA III had better results in terms of RMSE and correlation *R* than LARGO and EM38. The main limitation of this article was the sole surface condition being grassland. It is expected that by applying the sensing technologies over various types of vegetation a more extensive comparison will be performed in the future. Other limitations include the retrieval model used for the EM38, which has been shown in other studies to provide soil moisture to depths of 1.2 m or deeper. Improvement for EM38 may also include a more careful selection of the site which may minimise the impacts of spatial variation of clay, salt and organic matter upon conductivity measures (i.e., the ion content and distribution does not change much).

The correlation between corrected coherent reflectivity from LARGO and in situ soil moisture was not high enough due to the dry conditions of the field campaign. An independent retrieval algorithm to produce a LARGO-derived soil moisture product would not rely fully on ground measured soil moisture to determine the sensitivity to soil moisture variation, as has been done here. The development of mature electrodynamic models, alongside further analysis of *in situ* data, will provide more complete insight into how LARGO reflectivity can be used to retrieve soil moisture. The LARGO and EM38 systems mounted on this platform have an overall poor performance. Improvements including calibration methods, soil moisture retrieval algorithms, site selection, more data collection, etc., need to be made for a better soil moisture estimation in future studies.

ACKNOWLEDGMENT

The authors acknowledge the collaboration of a large number of scientists from throughout Australia and around the world, and in particular key personnel from the SMAP team which provided significant contribution to the campaign's design and execution. The authors would also like to acknowledge the contribution from Prof. Adriano Camps for the GNSS data processing. The ELBARA III and the LARGO instruments were provided by the Terrestrial Environmental Observatories and the Advanced Remote Sensing—Ground-Truth Demo and Test Facilities funded by the Helmholtz Association of German Research Centres (HGF). This article was perfomed within the SMAPEx framework.

REFERENCES

[1] W. Wagner *et al.*, "Evaluation of the agreement between the first global remotely sensed soil moisture data with model and precipitation data," *J. Geophys. Res. Atmos.*, vol. 108, no. D19, pp. 9-1–9-10, 2003.

[2] Y. Kerr, "Soil moisture from space: Where are we?," *Hydrogeol. J.*, vol. 15, no. 1, pp. 117–120, 2007.

[3] M. E. Holzman, R. Rivas, and M. C. Piccolo, "Estimating soil moisture and the relationship with crop yield using surface temperature and vegetation index," *Int. J. Appl. Earth Observ. Geoinf.*, vol. 28, no. 1, pp. 181–192, 2014.

[4] L. Rossato *et al.*, "Impact of soil moisture on crop yields over Brazilian semiarid," *Front. Environ. Sci.*, vol. 5, 2017.

[5] O. O. Aina, A. G. O. Dixon, and E. A. Akinrinde, "Effect of soil moisture stress on growth and yield of Cassava in Nigeria," *Pakistan J. Biol. Sci.*, vol. 10, no. 18, pp. 3085–3090, 2007.

[6] H. Carrão, S. Russo, G. Supulcre-Canto, and P. Barbosa, "An empirical standardized soil moisture index for agricultural drought assessment from remotely sensed data," *Int. J. Appl. Earth Observ. Geoinf.*, vol. 48, pp. 74–84, 2015.

[7] S. R. Evett, L. K. Heng, P. Moutonnet, and M. L. Nguyen, *Field Estimation of Soil Water Content: A Practical Guide to Methods, Instrumentation, and Sensor Technology*. Vinne, Austria: Int. Atomic Energy Agency, 2008.

[8] C. R. Hain *et al.*, "An intercomparison of available soil moisture estimates from thermal infrared and passive microwave remote sensing and land surface modeling," *J. Geophys. Res. Atmos.*, vol. 116, no. D15, 2011, Art. no. 15107.

[9] C. Rudiger *et al.*, "An intercomparison of ERS-Scat and AMSR-E soil moisture observations with model simulations over France," *J. Hydrometeorol.*, vol. 10, no. 2, pp. 431–447, 2009.

[10] E. G. Njoku, T. J. Jackson, V. Lakshmi, T. K. Chan, and S. V. Nghiem, "Soil moisture retrieval from AMSR-E," *IEEE Trans. Geosci. Remote Sens.*, vol. 41, no. 2, pp. 215–229, Feb. 2003.

[11] R. Panciera *et al.*, "Evaluation of the SMOS L-MEB passive microwave soil moisture retrieval algorithm," *Remote Sens. Environ.*, vol. 113, no. 2, pp. 435–444, 2009.

[12] H. Kim, V. Lakshmi, Y. Kwon, and S. V. Kumar, "First attempt of global-scale assimilation of subdaily scale soil moisture estimates from CYGNSS and SMAP into a land surface model," *Environ. Res. Lett.*, vol. 16, no. 7, 2021, Art. no. 074041.

[13] H. Kim and V. Lakshmi, "Use of cyclone global navigation satellite system (CYGNSS) observations for estimation of soil moisture," *Geophys. Res. Lett.*, vol. 45, no. 16, pp. 8272–8282, 2018.

[14] L. Gluba, M. Lukowski, R. Szlazak, K. Szewczak, and B. Usowicz, "Modelling of the soil moisture using L-band brightness temperatures from ELBARA III radiometer," in *Proc 12th Int. Conf. Electromagn. Wave Interaction Water Moist Substances*, 2018, pp. 1–9.

[15] M. Schwank *et al.*, "ELBARA II an L-band radiometer system for soil moisture research," *Sensors*, vol. 10, no. 1, pp. 584–612, 2010.

[16] F. Jonard, K. Z. J. L.Weihermüller, M. Schwank, H. Vereecken, and S. Lambot, "Mapping field-scale soil moisture with L-band radiometer and ground-penetrating radar over bare soil," *IEEE Trans. Geosci. Remote Sens.*, vol. 49, no. 8, pp. 2863–2875, Aug. 2011.

[17] T. Meyer, L. Weihermüller, H. Vereecken, and F. Jonard, "Vegetation optical depth and soil moisture retrieved from L-band radiometry over the growth cycle of a winter wheat," *Remote Sens.*, vol. 10, no. 10, 2018, Art. no. 1637.

[18] F. Jonard, L. Weihermüller, M. Schwank, K. Z. Jadoon, H. Vereecken, and S. Lambot, "Estimation of hydraulic properties of a sandy soil using ground-based active and passive microwave remote sensing," *IEEE Trans. Geosci. Remote Sens.*, vol. 53, no. 6, pp. 3095–3109, Jun. 2015.

[19] F. Jonard *et al.*, "Passive L-band microwave remote sensing of organic soil surface layers: A tower-based experiment," *Remote Sens.*, vol. 10, no. 2, 2018, Art. no. 304.

[20] T. J. Jackson *et al.*, " Soil moisture mapping at regional scales using microwave radiometry: The Southern Great Plains hydrology experiment," *IEEE Trans. Geosci. Remote Sens.*, vol. 37, no. 5, pp. 2136–2151, Sep. 1999.

[21] Y. H. Kerr *et al.*, "The SMOS mission: New tool for monitoring key elements ofthe global water cycle," *Proc. IEEE*, vol. 98, no. 5, pp. 666–687, May 2010.

[22] D. Entekhabi *et al.*, "The soil moisture active passive (SMAP) mission," *Proc. IEEE*, vol. 98, no. 5, pp. 704–716, May 2010.
[23] X. Wu, J. P. Walker, C. Rudiger, R. Panciera, and Y. Gao, "Intercomparison of alternate soil moisture downscaling algorithms using active-passive microwave observations," *IEEE Geosci. Remote Sens. Lett.*, vol. 14, no. 2, pp. 179–183, Feb. 2017.
[24] M. Martin-Neira, "A passive reflectometry and interferometry system (PARIS): Application to ocean altimetry," *ESA J.*, vol. 17, no. 4, pp. 331–355, 1993.
[25] V. U. Zavorotny and A. G. Voronovich, "Scattering of GPS signals from the ocean with wind remote sensing application," *IEEE Trans. Geosci. Remote Sens.*, vol. 38, no. 2, pp. 951–964, Mar. 2000.
[26] N. Rodriguez-Alvarez *et al.*, "Snow thickness monitoring using GNSS measurements," *IEEE Geosci. Remote Sens. Lett.*, vol. 9, no. 6, pp. 1109–1113, Nov. 2012.
[27] J. K. Stephen, T. Omar, S. G. Michael, and M. Dallas, "Utilizing calibrated GPS reflected signals to estimate soil reflectivity and dielectric constant: Results from SMEX02," *Remote Sens. Environ.*, vol. 100, no. 1, pp. 17–28, 2006.
[28] N. Rodriguez-Alvarez *et al.*, "Land geophysical parameters retrieval using the interference pattern GNSS-R technique," *IEEE Trans. Geosci. Remote Sens.*, vol. 49, no. 1, pp. 71–84, Jan. 2011.
[29] E. Alejandro *et al.*, "Global navigation satellite systems reflectometry as a remote sensing tool for agriculture," *Remote Sens.*, vol. 4, no. 12, pp. 2356–2372, 2012.
[30] A. Alonso-Arroyo *et al.*, "The light airborne reflectometer for GNSS-R observations (LARGO) instrument: Initial results from airborne and rover field campaigns," in *Proc. IEEE Geosci. Remote Sens. Symp.*, 2014, pp. 4054–4057.
[31] N. I. Huth and P. L. Poulton, "An electromagnetic induction method for monitoring variation in soil moisture in agroforestry systems," *Australian J. Soil Res.*, vol. 45, pp. 63–72, 2007.
[32] J. N. Stanley, D. W. Lamb, G. Falzon, and D. A. Schneider, "Apparent electrical conductivity (ECa) as a surrogate for neutron probe counts to measure soil moisture content in heavy clay soils (Vertosols)," *Soil Res.*, vol. 52, pp. 373–378, 2014.
[33] J. N. Stanley, D. W. Lamb, S. E. Irvine, and D. A. Schneider, "The effect of aluminium neutron probe access tubes on the apparent electrical conductivity recorded by an electromagnetic soil survey sensor," *IEEE Geosci. Remote Sens. Lett.*, vol. 11, no. 1, pp. 333–336, Jan. 2014.
[34] N. Ye *et al.*, "The soil moisture active passive experiments (SMAPEx): Validation of the SMAP products in Australia," *IEEE Trans. Geosci. Remote Sens.*, vol. 59, no. 4, pp. 2922–2939, Apr. 2021.
[35] O. Merlin *et al.*, "Calibration of a soil moisture sensor in heterogeneous terrain with the national airborne field experiment (NAFE) data," in *MODSIM 2007 International Congress On Modelling and Simulation*, Oxley, L. and Kulasiri, D. Eds., Canberra, ACT, Australia: Model. Simul. Soc. Australia, 2007, pp. 2604–2610.
[36] M. Chen and F. Z. Weng, "Modeling land surface roughness effect on soil microwave emission in community surface emissivity model," *IEEE Trans. Geosci. Remote Sens.*, vol. 54, no. 3, pp. 1716–1726, Mar. 2016.
[37] R. A. M. deJeu, T. R. H. Holmes, R. Panciera, and J. P. Walker, "Parameterization of the land parameter retrieval model for L-band observations using the NAFE'05 data set," *IEEE Geosci. Remote Sens. Lett.*, vol. 6, no. 4, pp. 630–634, Oct. 2009.
[38] Y. Gao *et al.*, "Evaluation of the tau–omega model for passive microwave soil moisture retrieval using SMAPEx datasets," *IEEE J. Sel. Topics Appl. Earth Observ. Remote Sens.*, vol. 11, no. 3, pp. 888–895, Mar. 2018.
[39] J. P. Wigneron *et al.*, "L-band microwave emission of the biosphere (L-MEB) model: Description and calibration against experimental data sets over crop fields," *Remote Sens. Environ.*, vol. 107, no. 4, pp. 639–655, 2007.
[40] P. O'Neill, S. Chan, E. Njoku, T. Jackson, and R. Bindlish, "Algorithm theoretical basis document: SMAP Level 23 soil moisture (passive)," 2012. [Online]. Available: http://smap.jpl.nasa.gov/files/smap2/L2&3_SM_P_InitRel_v1_filt2.pdf
[41] A. Alonso-Arroyo *et al.*, "An airborne GNSS-R field experiment over a vineyard for soil moisture estimation and monitoring," in *Proc. IEEE Int. Geosci. Remote Sens. Symp.*, 2015, pp. 4761–4764.
[42] J. D. McNeill, "Electromagnetic terrain conductivity measurement at low induction number," Geonics Limited, Mississauga, ON, Canada, Tech. Rep. TN-6, 1980.
[43] B. Hossain, "EM38 for measuring and mapping soil moisture in a cracking clay soil," Ph.D. thesis, School Sci. Technol., Univ. New England, 2008. [Online]. Available: https://hdl.handle.net/1959.11/2534

Xiaoling Wu received the B.E. degree in biomedical engineering from Zhejiang University, Hangzhou, China, in 2009, and the Ph.D. degree in civil engineering from Monash University, Melbourne, VIC, Australia, in 2015.

The topic of her undergraduate thesis was development of biosensor using nanomaterial. From 2009 to 2010, she was a Visiting Scholar with the Department of Computer Science, University of Copenhagen, Copenhagen, Denmark. The topic of her Ph.D. research was downscaling of soil moisture using airborne radar and radiometer observations in order to provide an accurate and high-resolution (better than 10 km) soil moisture product with potential benefit in the areas of weather forecasting, flood, and drought prediction, agricultural activities, etc. She is currently a Research Fellow with Monash University, Subang Jaya, Malaysia, and continuing high-resolution soil moisture work. Her research interests include microwave remote sensing of soil moisture, soil moisture downscaling, and proximal soil moisture sensing for real-time agricultural applications.

Jeffrey P. Walker received the B.E. in civil engineering and B. Surveying degrees in 1995 with Hons 1 and University Medal and the Ph.D. degree in water resources engineering from the University of Newcastle, Callaghan, NSW, Australia, in 1999.

His Ph.D. thesis was among the early pioneering research on estimation of root-zone soil moisture from assimilation of remotely sensed surface soil moisture observations. He was with NASA Goddard Space Flight Centre to implement his soil moisture work globally. In 2001, he was as a Lecturer with the Department of Civil and Environmental Engineering, University of Melbourne, where he continued his soil moisture work, including development of the only Australian airborne capability for simulating new satellite missions for soil moisture. In 2010, he was a Professor with the Department of Civil Engineering, Monash University, Melbourne, VIC, Australia, where he is continuing this research. He is contributing to soil moisture satellite missions at NASA, ESA and JAXA, as a Science Team Member for the Soil Moisture Active Passive mission and Cal/val Team Member for the Soil Moisture and Ocean Salinity and Global Change Observation Mission –Water, respectively.

François Jonard received the M.Sc. and Ph.D. degrees in bioscience engineering from the University of Louvain (UCLouvain), Louvain-la-Neuve, Belgium, in 2002 and 2012, respectively.

From 2006 to 2009, he was a Project Manager with different consultancy companies specialized in water resource management, geographic information systems, and remote sensing of the environment. From 2009 to 2021, he was a Researcher with the Institute of Bio- and Geosciences (Agrosphere), Research Center Jülich, Jülich, Germany. In 2011, he was a Visiting Scientist with the NASA Goddard Space Flight Center, Greenbelt, MD, USA, contributing to the preparation of the Soil Moisture Active and Passive mission. Since 2018, he has been a Regular Visiting Scientist with the Massachusetts Institute of Technology, Cambridge, MA, USA. His research interests include terrestrial remote sensing, ecosystem modelling, ecohydrology, and hydrogeophysics.

Dr. Jonard has been an Associate Professor with the Earth Observation and Ecosystem Modelling Laboratory and with the Faculty of Sciences, University of Liège, Liège, Belgium. He is also a Guest Professor with the Faculty of Bioscience Engineering, UCLouvain. Since 2021, he has been the recipient of the MIT-MISTI grant for early detection of plant water stress using remote sensing.

Nan Ye received the B.E. degree in hydraulic and hydropower engineering from Tsinghua University, Beijing, China, in 2006, and the Ph.D. degree in civil engineering from Monash University, Melbourne, VIC, Australia, in 2014.

Then, he coordinated a number of airborne field experiments for the in-orbit calibration/validation of the Soil Moisture Active Passive mission in the Murrumbidgee River catchment, southeast of Australia. He is currently a Research Fellow with Monash Suzhou Science and Technology Research Institute working on P-band passive microwave remote sensing of soil moisture.